Materials Transactions, Vol. 53, No. 3 (2012) pp. 565 to 570

EXPRESS REGULAR ARTICLE

Bone Loss and Reduced Bone Quality of the Human Femur after Total Hip Arthroplasty under Stress-Shielding Effects by Titanium-Based Implant

Yoshihiro Noyama[1,2,*1], Takuya Miura[1,*1], Takuya Ishimoto[1], Takahiro Itaya[1,*1], Mitsuo Niinomi[3] and Takayoshi Nakano[1,*2]

[1]*Division of Materials and Manufacturing Science, Graduate School of Engineering, Osaka University, Suita 565-0871, Japan*
[2]*Department of Research and Development Division, Nakashima Medical Co., Ltd., Okayama 709-0625, Japan*
[3]*Department of Biomaterials Science, Institute for Materials Research, Tohoku University, Sendai 980-8577, Japan*

The present work was aimed at clarifying the stress-shielding effect caused by hip-joint implantation into a femur by using a human cadaver with a cementless hip implant. In particular, bone quality was assessed from the standpoint of preferential *c*-axis orientation of biological apatite (BAp). Comparing the implanted side to the non-implanted side, a finite element analysis (FEA) indicated that artificial hip-joint implantation had a significant stress-shielding effect on the femur. The results also showed a marked decrease in the degree of preferential BAp orientation as well as bone loss in the medial-proximal femur. This is the first report showing a reduction in the degree of preferential BAp orientation due to a stress-shielding effect after artificial hip-joint implantation. Since preferential BAp orientation is an important index for determining bone mechanical function, these findings should be taken into account in future artificial hip-joint designs, especially those involving the stem component. [doi:10.2320/matertrans.M2011358]

(Received November 21, 2011; Accepted December 19, 2011; Published February 15, 2012)

Keywords: *titanium, biomaterial, total hip arthroplasty, stress-shielding effect, biological apatite (BAp), preferential orientation, bone quality, finite element analysis (FEA)*

1. Introduction

Total hip replacement (THR) is an orthopedic surgical procedure to reconstruct a hip joint that has lost its function due to severe bone or joint disease, such as osteoarthritis or rheumatoid arthritis. The number of THR procedures performed worldwide has been increasing yearly, with 231,000 such operations taking place in 2006 in the United States.[1)] However, artificial hip-joint implantation leads to bone resorption of the surrounding femur, reducing bone strength and leading to a high rate of fractures.[2)] One of the evidences can be seen in the fact that in the United States, periprosthetic fractures are factors in 18.7% of artificial hip-joint recipients showing revisions to the femoral component.[3)] Thus, implants that are intended to restore hip-joint function are themselves causing serious problems such as bone deterioration and loss of bone function. Bone loss due to stress-shielding effects is believed to be the main cause of such periprosthetic fractures.[4)] The stress-shielding effect is a phenomenon in which *in vivo* applied stress bypasses the surrounding bone, resulting in a preferential load on to an implant with a high Young's modulus and an inhibition of the normal stress transfer to the surrounding bone. Artificial hip joints of varying materials, structural properties, and surface treatments have been investigated for their ability to reduce the stress-shielding effect.[2)] Most of the works have used bone mass or bone mineral density (BMD) as indices of the stress-shielding effect.

Bone mechanical function is directly associated with bone fracture risk and is influenced by bone mass, BMD, and bone quality.[5)] Bone quality refers to factors other than bone mass and BMD that contribute to bone mechanical function. However, most articles discussing the stress-shielding effect from implant implantation have not investigated the bone quality. This work therefore focused on the degree of preferential *c*-axis orientation of biological apatite (BAp) as a measure of bone quality. The mechanical function of bone tissue is determined by the degree of preferential orientation of BAp,[6)] which is based on the anisotropic mechanical properties of BAp.[7)] In addition, the degree of preferential *c*-axis orientation of BAp is established along the direction of principal stress loaded on the bone.[8)] For example, in the cortical bone portion of the mandibles of monkeys and beagles, the *c*-axis of BAp is basically oriented uniaxially along the mesiodistal axis. However, in the vicinity of the teeth and dental roots that bear the load during mastication, the orientation sensitively changes toward the direction of mastication.[8,9)] Therefore, degree of preferential BAp orientation can be a useful evaluation index of the stress-shielding effect caused by implant insertion. It can also be an important bone quality index for estimating bone mechanical function and fracture risk of the femur surrounding an artificial hip joint. It has been reported that insertion of a nail into the tibial marrow cavity of rabbits reduced the degree of preferential BAp orientation of the cortical bone of the tibia.[10)] However, according to our knowledge, there has been no report of an actual clinical example describing the influence the stress-shielding effect of artificial hip-joint implantation has on the degree of BAp orientation in the surrounding femur.

Bone loss due to the stress-shielding effect has been reported to be site-dependent. Using the Gruen zones (see Fig. 1) as the standard,[11)] bone loss at proximal sites, such as zones 1, 2, 6 and 7, has been reported to be greater than that at the other sites.[12,13)] Among these, the medial-proximal

*[1]Graduate Student, Osaka University
*[2]Corresponding author, E-mail: nakano@mat.eng.osaka-u.ac.jp

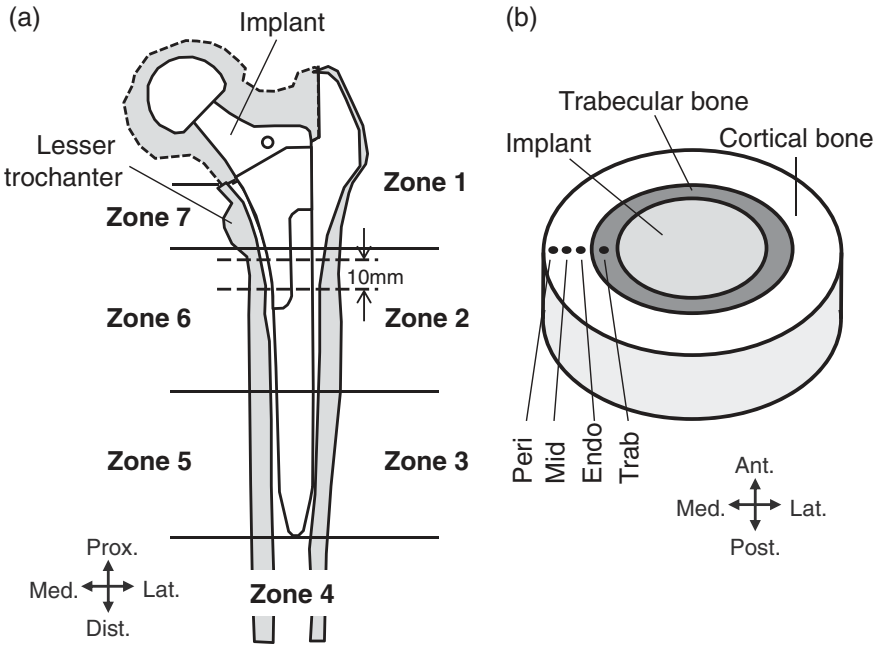

Fig. 1 (a) Schematic diagram of sample preparation from the proximal region of a human femur. (b) Analyzed region in a cross-section excised from the femur (zones 2 and 6) as shown in (a). The Gruen zones are also drawn in this figure.

zones 7 and 6 (zone 7 is the more proximal) are important medial sites for fixing cementless artificial hip joints.[14] Therefore, adequate stress transfer at these sites could effectively prevent the stress-shielding effect. The medial-proximal femur, to which the artificial hip joint made of titanium alloy is applied, is the most appropriate site for elucidating the influence of the stress-shielding effect on the degree of BAp orientation.

This work investigated an artificial hip joint applied to the medial-proximal femur in a human cadaver. The stress-shielding effect caused by artificial hip-joint implantation was estimated to determine its influence on bone mass and bone quality assessed by the degree of BAp orientation.

2. Materials and Methods

2.1 Bone samples

The right and left femurs from the human cadaver of an 80-year-old man (provided by the Osaka City University Hospital) were used. The samples were fixed in 10% neutral-buffered formalin to prevent infection and degeneration of organic material. The left femur had a metallic cementless artificial hip joint (VerSys® HA/TCP FiberMetalTaper, Zimmer, USA), and there was no implant on the right femur. Thus, the left femur was the implant side and the right femur was the control side. The length of time the implant had been inserted was not made available for reasons of personal privacy.

The femoral stem and head components of the artificial hip joint were composed of Ti–6Al–4V alloy and Co–Cr–Mo alloy (Zimaloy), respectively. Surface treatment of the implant included the use of a titanium mesh on the proximal region to induce osteoconduction, hydroxyapatite (HAp) and tricalcium phosphate (TCP) coating on the medial region, and a mirror finish on the distal region.

As shown in Fig. 1, a 10-mm section beginning immediately below the lesser trochanter on the distal side was excised with a micro cutter (BS-300CP; Exakt Apparatebeau, Norderstedt, Germany). The medial region of the block was used to analyze bone mass and the degree of BAp orientation. To analyze the BAp orientation, the cross-sectional surface of the medial region of the region immediately below the lesser trochanter was polished with emery paper up to 2,000 grit. The region immediately below the lesser trochanter was located at the border of Gruen zones 6 and 7.

2.2 Analysis of bone mass and bone quality

Based on the Gruen classification,[11] the femur was placed in a position equivalent to the supine position, and X-ray images were taken with a 400 kV tube voltage and a 100 mA tube current (X'sy, Shimadzu, Japan). BMD was also measured in the supine position using a dual-energy X-ray absorptiometer (DXA) (DCS-600EX, Hitachi Aloka Medical, Japan). Three-dimensional (3D) images of the analyzed region were obtained by micro-focus X-ray computed tomography (μCT) (SMX-100CT-SV3, Shimadzu, Japan) with a tube voltage of 70 kV and a tube current of 50 μA. Spatial resolution was set to $30.5 \times 30.5 \times 30.5\ \mu m^3$. The 3D images were binarized by using software for the analysis of bone microstructure (3D-BON, RATOC, Japan), which was used to calculate the ratio of bone volume to total tissue volume (Bone Volume/Tissue Volume, BV/TV). To quantitatively evaluate the degree of BAp orientation, (002) and (310) diffraction peaks of BAp parallel to the longitudinal bone axis of the femur were obtained using a microbeam X-ray diffractometer (XRD) (D8 Discover with GADDS; Bruker AXS, Germany) with a reflective optical system and a Cu-$K\alpha$ line with a tube voltage of 45 kV and a tube current of 110 mA. The degree of BAp c-axis orientation was determined by calculating the (002)/(310) intensity ratio. The

incident X-ray beam was focused to 100 μm in diameter by a monocapillary collimator, and the angle of incidence oscillated from 13 to 20 degrees. The measurement time was set to 1,800 s. Since a randomly oriented hydroxyapatite (HAp) powder shows an integrated intensity ratio of 0.6, an integrated intensity ratio greater than this non-orientation value suggests a preferential *c*-axis orientation parallel to the long axis of the femur. For measurements of the degree of BAp orientation, the medial cortical bone was divided into 3 regions in the direction of the thickness (from periosteal side to endosteal side: "Peri", "Mid" and "Endo"), and the average of 3 measurements from the central areas of each region was used as data. BV/TV was analyzed at 4 regions in the cortical ("Peri", "Mid" and "Endo") and trabecular bones (Trab) [see Fig. 1(b)].

2.3 Stress simulation

To predict the stress-shielding effect after artificial hip-joint implantation, stress simulation was conducted using a finite element analysis (FEA). 3D bone models used for the stress simulation were prepared as follows. Tomographic images of the femur were obtained by using a medical CT system (ECLOS 4S, Hitachi Medico, Japan) with a tube voltage of 120 kV, a tube current of 150 mA, and a slice width of 1.25 mm. Each CT image was binarized, and the cortical bone was extracted using CT image analysis software (Mimics 11, Materialise, Belgium). A 3D model of the femur was constructed on the basis of the layered contour using 3D surface modeling software (Imageware 10, SIEMENS, USA).[15] For the implant model, images of the artificial hip-joint configuration were reproduced using 3D CAD software (SolidWorks 2006, SolidWorks, USA), and these images were combined with the femur model by matching them with soft X-ray radiographs taken in multiple directions. The 4 elements of the combined model were defined as the implant portion, cortical bone portion, trabecular bone portion, and bone marrow portion (Fig. 2). FEA was performed using non-linear analysis software (MSC.Marc 2008, MSC Software, USA). Primary tetrahedral elements were used as the finite elements with 928,915 elements and 173,098 nodes. The loading conditions were based on the method proposed by Akay *et al.*,[16] in which the force placed on a human hip joint while walking at 1 km/h is divided into 3 components. F1 is the force parallel to the femoral axis on the femoral head (1,850 N in the distal direction, 785 N from the medial direction, and 17.5 N from the anterior direction); F2 is the force parallel to the femoral axis on the greater trochanter (967 N in the proximal direction, 471 N from the lateral direction, and 144 N from the anterior direction). At the boundary of the implant, the titanium mesh was completely fixed to the bone, the implant surfaces were polished to ensure that no bone was attached to other bone-implant interfaces, and the surface of the femur model's inferior extremity was completely immobilized. Table 1 shows the Young's modulus and Poisson ratio for each element. On the implant side, Ti–6Al–4V alloy (114 GPa, 0.3) and Co–Cr–Mo alloy (210 GPa, 0.3)[17] were used. On the bone side, cortical bone (16 GPa, 0.3), trabecular bone (1 GPa, 0.3), and bone marrow (0.3 GPa, 0.45)[18,19] were used. Maximum principal stress was quantified at regions where the BV/TV and BAp orientation were measured. For quantification data, 2-tailed Student's *t*-tests were used to compare mean values, and $P < 0.05$ was considered statistically significant.

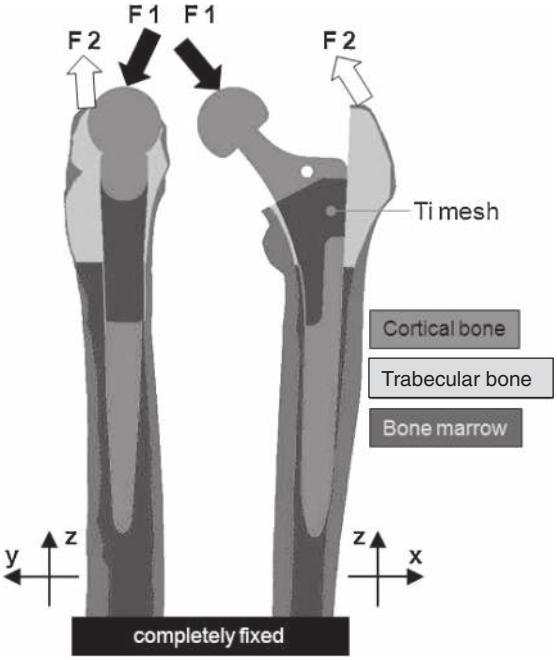

Fig. 2 Schematic diagram of the finite element analysis (FEA) model, loading conditions, and constraining conditions.

Table 1 Physical properties of each element used in the FEA.

Part	Material	Young's modulus /GPa	Poisson's ratio
Head	Co–Cr–Mo alloy	210	0.3
Femoral stem	Ti–6Al–4V alloy	114	0.3
Cortical bone	Cortical bone	16	0.3
Trabecular bone	Trabecular bone	1	0.3
Bone marrow	Bone marrow	0.3	0.45

3. Results

Figure 3(a) shows the maximum principal stress distribution in the femur cross-section immediately inferior to the lesser trochanter, as analyzed by FEA. Compressive principal stress parallel to the femoral axis was dominant in all regions. Figure 3(b) shows the maximum principal stress in the Peri, Mid and Endo regions of the medial part. Artificial hip-joint implantation significantly reduced applied stress values in all regions. The stress difference was particularly large in the Peri region, suggesting that this is the location of the marked stress-shielding effect.

Figure 4 shows an X-ray radiograph in an anterior–posterior projection. On the implant side, cortical bone radiopacity declined in the vicinity of the medial-proximal lesser trochanter, indicating the bone resorption. The BMD was 2.21 g/cm^2 on the control side and 1.87 g/cm^2 on the implant side, a reduction of approximately 15%. CT images are shown in Fig. 5(a). The endosteal region of the cortical bone was markedly more porous on the implant side.

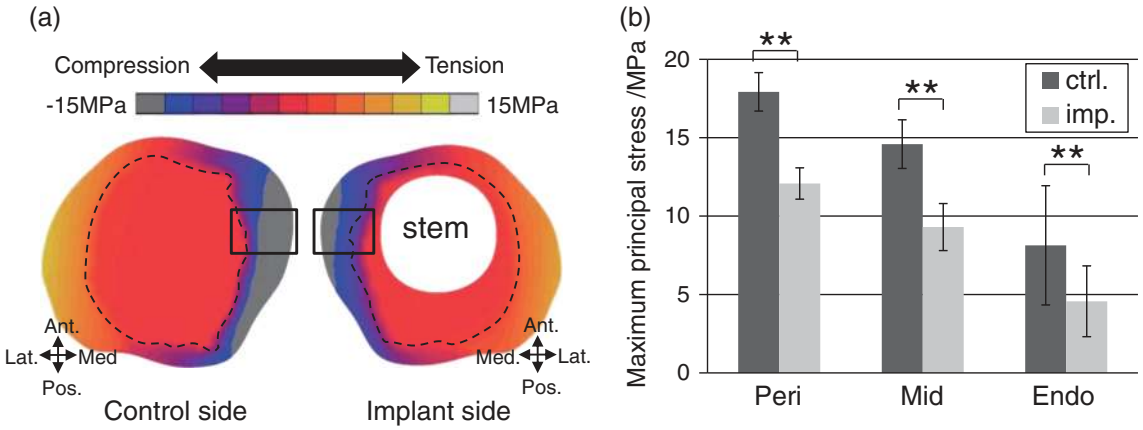

Fig. 3 (a) Comparison of the maximum principal stress distributions in the cross section of the proximal region of the femur shown in Fig. 1(b) in the presence and the absence of an artificial hip joint. (b) Comparison of the maximum principal stress values at 3 regions (Peri, Mid and Endo) along the direction of the thickness of the bone in the medial region. Broken lines mean the boundary between cortical and trabecular regions. Asterisks (**) indicate *P*-value of $P < 0.01$.

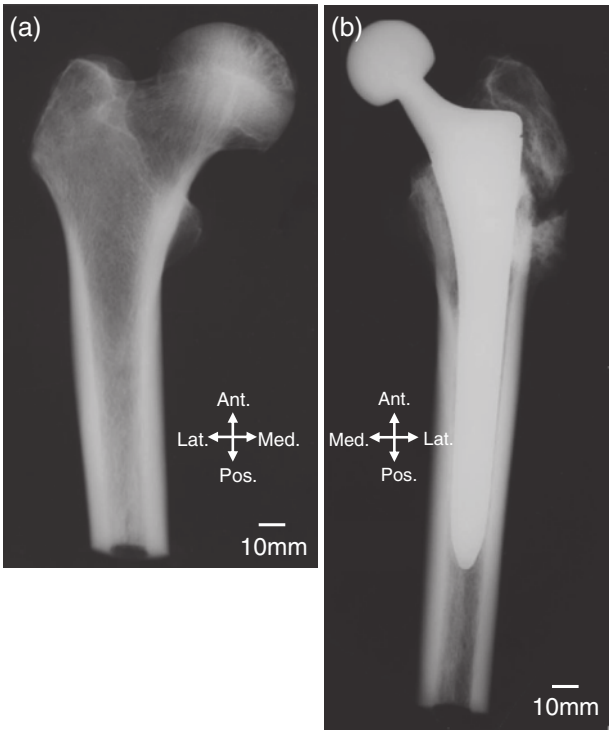

Fig. 4 Anteroposterior projection X-ray radiographs of a human femur (a) without and (b) with an artificial hip joint.

Quantification of BV/TV of the cortical bone portion and the trabecular bone portion is shown in Fig. 5(b), which shows a significant decrease in BV/TV in all regions except for the Peri region. Bone loss was particularly pronounced in the vicinity of the endosteum.

As shown in Fig. 6, the degree of BAp *c*-axis orientation along the longitudinal axis of the femur showed numerical values higher than 0.6 at all regions in both the left and right femurs, indicating that the preferential BAp orientation was parallel to the longitudinal direction of the femur. Values in the Peri region of the implant side were significantly lower than those in the control side, but there were no significant differences between the two sides in the Mid and Endo regions.

4. Discussion

This work examined the influence of the stress-shielding effect caused by artificial hip-joint implantation on bone mass and bone quality (preferential BAp orientation) of the surrounding femur. It was found that artificial hip-joint implantation caused a marked stress-shielding effect, resulting in significant bone loss and reduced bone quality in the femoral cortical bone. This article is the first to describe the influence of the stress-shielding effect on preferential BAp orientation.

The stress-shielding effect caused a remarkable progression of bone loss on the side of the femoral endosteum and led to change the cortical bone into the trabecular-like bone. There was no significant bone loss on the periosteal side (Fig. 5). This is consistent with previous reports demonstrating that the femoral endosteal diameter enlarges after implantation of a cementless artificial hip joint, while the periosteal diameter remains unchanged.[20] This may be attributable to bone functional adaptation via osteonal remodeling in a stress-shielding environment on the endosteal side.[21] As a result, the periosteal side ultimately remains intact. However, the degree of BAp orientation in the longitudinal direction was significantly reduced on the periosteal side (Fig. 6). The degree of preferential BAp orientation is related to bone mechanical function, and reduced orientation is an important contributor to reduced bone mechanical function.[7,22] In fact, Ni *et al.*[23] reported that the micro-hardness in the region proximal to the artificial hip joint is 20% lower than that on the non-implanted side. This may suggest that the change in the degree of BAp orientation is involved in this phenomenon. In other words, reduction in bone mechanical function and fracture risk in the femur after artificial hip-joint implantation were greater than the values predicted by considering bone loss alone, thereby suggesting that the reduced degree of BAp orientation on the periosteal side played a role in this deterioration in bone function.

Preferential BAp orientation varies depending on the direction or magnitude of the principal stress.[8] Accordingly, this suggests its functional adaptation is optimally mediated by external loads, similar to the scenario in the case of bone

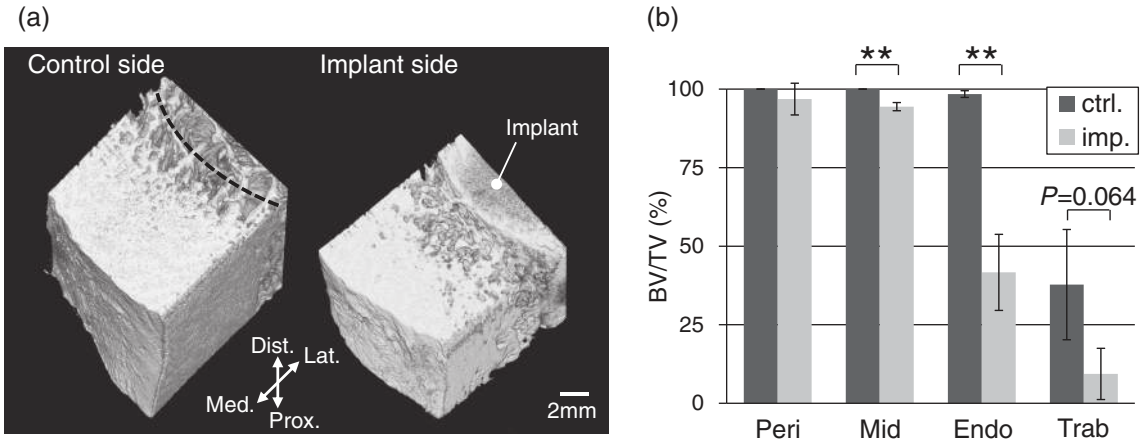

Fig. 5 (a) Comparison of μCT-3D images taken of the medial proximal femur. (b) Bone volume fraction (BV/TV) at the 4 regions (Peri, Mid, Endo and Trab) shown in Fig. 1(b). The asterisks (**) indicate a *P*-value of $P < 0.01$.

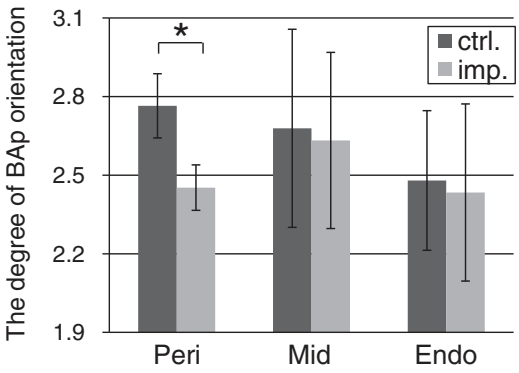

Fig. 6 Distribution of the degree of BAp orientation at the 3 cortical bone regions (Peri, Mid and Endo) shown in Fig. 1(b). The asterisks (*) indicate a *P*-value of $P < 0.05$.

mass and bone density. In a non-stress environment after removal of the ulna mid-diaphysis of a rabbit, a significant reduction in the degree of BAp orientation in the remaining portion of the ulna was observed.[24] This suggests that stress shielding of the bone caused by an artificial hip joint is a critical factor not only in bone loss, but also in the degradation of bone quality.

Various types of artificial hip joints have been designed to reduce stress-shielding effect and prevent bone loss and reduced bone quality. The artificial hip joint, which made of titanium alloy, used in this work was proximally coated with titanium mesh[25] to promote osseointegration through bone in-growth, and to transfer stress between the stem and the bone. However, a large portion of the trabecular bone in the medial-proximal femur, which is ideally attached with the implant and plays an important role in stress transfer to the cortical bone, was lost in the implanted femur (Fig. 5). This provides evidence that stress was not sufficiently transferred to the cortical bone, causing stress-shielding effect. Meanwhile, direct measurements of deformations using a cadaver[26] and FEA[14] have shown that a low Young's modulus of the material decreases stress-shielding effect to the surrounding femur. However, it is impossible to completely eliminate stress-shielding effects, even with a stem made of polymethylmethacrylate with a very low Young's modulus (1.9 GPa).[26] Therefore, in addition to conventional methods, it is important to develop new concepts in the design of artificial hip joints to prevent stress shielding. If, for example, the material and shape of implants can be optimized to actively transfer stress from the artificial hip joint to the bone through the effective use of functional adaptations,[27] it may be possible to produce artificial hip joints that do not cause stress shielding, reduce bone function, or lead to periprosthetic fractures.

In addition, making bone quality a standard for bone assessments could play in important role in implant design. Unlike bone mass and bone density, bone quality has not been taken into account in the design of artificial hip joints and evaluation of the stress-shielding effect. The effectiveness of various indicators of bone quality has been previously examined in the treatment of metabolic bone diseases such as osteoporosis and in the evaluation of bone mechanical function.[28] Among these, the preferential orientation of BAp has been shown to be an effective indicator of clinical conditions in bone diseases.[29] It has also been shown to be a promising material property index of cortical bone in the evaluation of the pharmacological efficacy of osteoporosis drugs in animal experiments.[30] We are currently investigating artificial-joint design using the degree of preferential orientation of BAp as an index.

5. Conclusions

This work analyzed the stress-shielding effect in the medial-proximal human femur implanted with a cementless artificial hip joint using parameters of bone mass and the degree of BAp *c*-axis orientation, which is closely related to bone mechanical function. The key findings are as follows:

(1) A marked stress-shielding effect was observed in the medial-proximal human femur after artificial hip-joint implantation.

(2) The stress-shielding effect resulted in bone resorption and bone loss. Bone loss was especially pronounced in the trabecular bone between the femoral stem and the cortical bone, as well as in the vicinity of the endosteum of the cortical bone, but was not significant in the periosteal region of the cortical bone.

(3) The stress-shielding effect significantly decreased preferential BAp orientation in the periosteal region. Because these changes are based on the bone functional adaptation to a reduced stress, it is important to design artificial hip joints that actively promote stress loading onto the surrounding bone. This could help suppress the stress-shielding effect, thus preventing bone loss and the degradation of degree of BAp orientation.

Acknowledgments

This work was supported by the Funding Program for Next Generation World-Leading Researchers from the Japan Society for the Promotion of Science (JSPS) and the "Super Special Consortia" for supporting the development of cutting-edge medical care (Cabinet office, Government of Japan; Ministry of Health, Labor and Welfare; Ministry of Education, Culture, Sports, Science, and Technology; and Ministry of Economy, Trade, and Industry). We thank Prof. H. Iwaki and Prof. A. Kobayashi of Graduate School of Medicine, Osaka City University for useful comments and discussion. We thank Prof. Y. Nakajima and Prof. H. Kiyama of Graduate School of Medicine, Osaka City University for providing the bone specimen. Finally, we thank the donor's family for their generosity.

REFERENCES

1) National Hospital Discharge Survey: 2006 annual summary, (U.S. Department of Health and Human Services, 2010).
2) J. W. Harkess: *Campbell's Operative Orthopaedics*, 11th ed., S. T. Canale and J. H. Beatty eds. (Mosby Elsevier, 2007) chapter 7.
3) K. J. Bozic, S. M. Kurtz, E. Lau, K. Ong, T. P. Vail and D. J. Berry: J. Bone Joint Surg. Am. **91** (2009) 128–133.
4) H. Lindahl: Injury **38** (2007) 651–654.
5) NIH Consensus Development Panel on Osteoporosis Prevention, Diagnosis, and Therapy: JAMA **285** (2001) 785–795.
6) W. Bonfield and M. D. Grynpas: Nature **270** (1977) 453–454.
7) B. Viswanath, R. Raghavan, U. Ramamurty and N. Ravishankar: Scr. Mater. **57** (2007) 361–364.
8) T. Nakano, K. Kaibara, Y. Tabata, N. Nagata, S. Enomoto, E. Marukawa and Y. Umakoshi: Bone **31** (2002) 479–487.
9) W. Fujitani and T. Nakano: Mater. Sci. Forum **654–656** (2010) 2216–2219.
10) T. Nakano, T. Kan, T. Ishimoto, Y. Ohashi, W. Fujitani, Y. Umakoshi, T. Hattori, Y. Higuchi, M. Tane and H. Nakajima: Mater. Trans. **47** (2006) 2233–2239.
11) T. A. Gruen, G. M. McNeice and H. C. Amstutz: Clin. Orthop. Rel. Res. **141** (1979) 17–27.
12) G. Sköldenberg, H. S. G. Bodén, M. O. F. Salemyr, T. E. Ahl and P. Y. Adolphson: Acta Orthop. **77** (2006) 386–392.
13) J. Kärrholm, C. Anderberg, F. Snorrason, J. Thanner, N. Langeland, H. Malchau and P. Herberts: J. Bone Joint Surg. Am. **84A** (2002) 1651–1658.
14) R. Huiskes, H. Weinans and B. V. Rietbergen: Clin. Orthop. Rel. Res. **274** (1992) 124–134.
15) B. Mahaisavariya, K. Sitthiseripratip, T. Tongdee, E. L. J. Bohez, J. V. Sloten and P. Oris: Med. Eng. Phys. **24** (2002) 617–622.
16) M. Akay and N. Aslan: J. Biomed. Mater. Res. **31** (1996) 167–182.
17) A. W. L. Turner, R. M. Gillies, R. Sekel, P. Morris, W. Bruce and W. R. Walsh: J. Orthop. Res. **23** (2005) 705–712.
18) T. P. Harrigan, J. A. Kareh, D. O. O'Connor, D. W. Burke and W. H. Harris: J. Orthop. Res. **10** (1992) 134–144.
19) A. Schonning, B. Oommen, I. Ionescu and T. Conway: Comput. Aided Des. **41** (2009) 566–572.
20) P. Adolphson: J. Arthroplasty **11** (1996) 572–581.
21) B. Busse, M. Hahn, T. Schinke, K. Püschel, G. N. Duda and M. Amling: J. Biomed. Mater. Res. A **92** (2010) 1440–1451.
22) T. Ishimoto, T. Nakano, M. Yamamoto and Y. Tabata: J. Mater. Sci. Mater. Med. **22** (2011) 969–976.
23) G. X. Ni, W. W. Lu, P. K. Y. Chiu, Y. Wang, Z. Y. Li, Y. G. Zhang, B. Xu, L. F. Deng and K. D. K. Luk: J. Orthop. Res. **25** (2007) 1408–1414.
24) T. Ishimoto, T. Nakano, Y. Umakoshi, M. Yamamoto and Y. Tabata: Phosphorus Res. Bull. **17** (2004) 77–82.
25) T. H. Mallory and W. C. Head: Contemp. Orthop. **17** (1988) 21–28.
26) T. P. Vail, R. R. Glisson, T. D. Koukoubis and F. Guilak: J. Biomech. **31** (1998) 619–628.
27) Y. Noyama, N. Nagayama, T. Ishimoto, K. Kuramoto, T. Sakai, H. Yoshikawa and T. Nakano: Mater. Sci. Forum **638–642** (2010) 664–669.
28) C. J. Hernandez and T. M. Keaveny: Bone **39** (2006) 1173–1181.
29) J. W. Lee, T. Nakano, S. Toyosawa, Y. Tabata and Y. Umakoshi: Mater. Trans. **48** (2007) 337–342.
30) A. Shiraishi, S. Miyabe, T. Nakano, Y. Umakoshi, M. Ito and M. Mihara: BMC Musculoskelet. Disord. **10** (2009) paper #66.